Effects of platelet-rich plasma on mesenchymal stem cells isolated from rat uterus

Polina Vishnyakova [Corresp., Equal first author, 1, 2], **Daria Artemova** [Equal first author, 1], **Andrey Elchaninov** [1, 3], **Zulfiia Efendieva** [4], **Inna Apolikhina** [1, 4], **Gennady Sukhikh** [1], **Timur Fatkhudinov** [2, 5]

[1] National Medical Research Center for Obstetrics, Gynecology and Perinatology Named after Academician V.I. Kulakov of Ministry of Healthcare of Russian Federation, Moscow, Russia

[2] People' s Friendship University of Russia, Moscow, Russia

[3] Pirogov Russian National Research Medical University (RNRMU), Moscow, Russia

[4] I. M. Sechenov First Moscow State Medical University of Ministry of Health of Russia (Sechenov University), Moscow, Russia

[5] Scientific Research Institute of Human Morphology, Moscow, Russia

Corresponding Author: Polina Vishnyakova
Email address: vpa2002@mail.ru

Background. Platelet-rich plasma (PRP), which represents a valuable source of growth factors, is increasingly applied in regenerative medicine. Recent findings suggest the feasibility of using PRP for the treatment of the infertility caused by refractory thin endometrium. Mesenchymal stem/stromal cells (MSCs) of the endometrium are an essential cellular component responsible for the extracellular matrix remodeling, angiogenesis, cell-to-cell communication and postmenstrual tissue repair. In this study, we examine the effects of autologous PRP on the MSCs isolated from the uterus and compare them with the effects of autologous ordinary plasma (OP) and complete growth medium in rat model.

Methods. MSCs were isolated from the uterine tissues by enzymatic disaggregation. The flow cytometry immunophenotyping of the primary cell cultures was complemented with immunocytochemistry for Ki-67 and vimentin. The ability of MSCs to differentiate in osteo-, chondro- and adipogenic directions was assessed with the use of differentiation-inducing media. The levels of autophagy and apoptosis markers, as well as the levels of matrix metalloproteinase 9 (MMP9) and estrogen receptor α, were assessed by western blotting.

Results. After 24 h incubation, proliferation index of the PRP-treated MSC cultures was significantly higher compared with complete growth medium. PRP elevated production of LC3B protein, an autophagy marker, while OP upregulated the expression of stress-induced protein p53 and extracellular enzyme MMP9. The results indicate practical relevance and validity of PRP usage in the treatment of infertility.

Effects of platelet-rich plasma on mesenchymal stem cells isolated from rat uterus

Vishnyakova Polina [1,2#*], Artemova Daria [1#], Elchaninov Andrey [1,3], Efendieva Zulfiia[4], Apolikhina Inna [1,4], Sukhikh Gennady [1] and Fatkhudinov Timur [2,5]

Author affiliations:

[1] National Medical Research Center for Obstetrics, Gynecology and Perinatology Named after Academician V.I. Kulakov of Ministry of Healthcare of Russian Federation, Moscow, Russia

[2] Peoples' Friendship University of Russia, Moscow, Russia

[3] Pirogov Russian National Research Medical University (RNRMU)

[4] I. M. Sechenov First Moscow State Medical University of Ministry of Health of Russia (Sechenov University), Moscow, Russia

[5] Scientific Research Institute of Human Morphology, Moscow, Russia

# – equal contribution

Corresponding Author:

Polina A. Vishnyakova, PhD

Laboratory of regenerative medicine, Research Center for Obstetrics, Gynecology and Perinatology, Ministry of Healthcare of the Russian Federation, Moscow, Russia. Tel: +79150658577.

Email: vpa2002@mail.ru or vishnyakovapolina@gmail.com

Abstract

Background. Platelet-rich plasma (PRP), which represents a valuable source of growth factors, is increasingly applied in regenerative medicine. Recent findings suggest the feasibility of using PRP for the treatment of the infertility caused by refractory thin endometrium. Mesenchymal stem/stromal cells (MSCs) of the endometrium are an essential cellular component responsible for the extracellular matrix remodeling, angiogenesis, cell-to-cell communication, and postmenstrual tissue repair. In this study, we examine the effects of autologous PRP on the MSCs isolated from the uterus and compare them with the effects of autologous ordinary plasma (OP) and complete growth medium in rat model.

Methods. MSCs were isolated from the uterine tissues by enzymatic disaggregation. The flow cytometry immunophenotyping of the primary cell cultures was complemented with immunocytochemistry for Ki-67 and vimentin. The ability of MSCs to differentiate in osteo-, chondro- and adipogenic directions was assessed with the use of differentiation-inducing media. The levels of autophagy and apoptosis markers, as well as the levels of matrix metalloproteinase 9 (MMP9) and estrogen receptor α, were assessed by western blotting.

Results. After 24 h incubation, proliferation index of the PRP-treated MSC cultures was significantly higher compared with complete growth medium. PRP elevated production of LC3B protein, an autophagy marker, while OP upregulated the expression of stress-induced protein p53 and extracellular enzyme MMP9. The results indicate practical relevance and validity of PRP usage in the treatment of infertility.

Introduction

Platelet-rich plasma (PRP) is a term for collected blood plasma with artificially concentrated platelets (Theoret & Stashak, 2014) and correspondingly increased loads of latent growth factors and other active substances. Blood platelets contain three types of granules: dense granules, α-granules and lysosomes (Flaumenhaft & Sharda, 2018); the most abundant are α-granules which contain a number of active substances including chemokines and growth factors (Yun et al., 2016) e.g. platelet-derived growth factors (PDGFs), transforming growth factors (TGFs), insulin-like growth factors (IGFs), vascular endothelial growth factor (VEGF), epidermal growth factor (EGF), fibroblast growth factors (FGFs) (Lubkowska, Dolegowska & Banfi, 2012). PRP is also rich in fibrin, fibronectin and vitronectin (Marx, 2019). PRP as a potential therapeutics for tissue repair was introduced in 1998 by Marx et al. (Marx et al., 1998) who reported enhanced rates of

bone formation in the osteoplasty of human mandibular defects upon adding PRP to the milled bone graft. By now, PRP is widely used in cosmetology, dentistry, sports medicine and surgery (Yuksel et al., 2014; Maffulli, 2016; Patel et al., 2016); it can be injected in soft tissues, mixed with a graft, layered, sprayed, or used as a biological membrane (Civinini et al., 2011). Degranulation of the platelets upon the PRP activation promotes fibrinogen cleavage and formation of the gel-like matrix. Main PRP activators used in laboratory practice are calcium, thrombin and collagen (Cavallo et al., 2016; Maffulli, 2016). The most common PRP activator is calcium, which acts faster than collagen but slower than thrombin (Kim & Byeon, 2019). The activation leads to immediate release of growth factors which start to act at the site of PRP administration. The platelets release 70% of their total content of growth factors within 10 minutes after PRP activation with $CaCl_2$, and the rest 30% are released in the course of 1 hour. Moreover, the activated platelets continue to produce extra amounts of growth factors. As the activated platelets die at about 8 hours after the stimulus, PRP activation should be carried out immediately before the use (Kim & Byeon, 2019).

PRP exerts a local stimulating effect on cell growth at the site of administration. The benefits of PRP treatment are currently finding recognition in reproductive technologies. A recent study involved 24 female participants with refractory thin endometrium (5 mm or thinner) and a history of IVF failure: a course of three repeated infusions of PRP into the uterine cavity caused significant improvement in the condition, with, respectively, 60% of and 54% of the patients successfully entering pregnancy and giving birth (Frantz et al., 2020). The effectiveness of PRP for the treatment of the thin endometrium has been previously reported by Zadehmodarres et al.; the study involved 10 female participants with thin endometrium (7 mm or thinner) who received PRP infusions. After two infusions, the thickness of endometrium exceeded 7 mm in all patients,

which enabled the frozen-thawed embryo transfer (FET) procedure. As a result, 5 (50%) of the patients successfully entered pregnancy (Zadehmodarres et al., 2017). Coksuer et al. evaluated the PRP treatment of thin endometrium as an alternative to estradiol therapy in patients with a history of three or more failed IVF cycles. The resulting endometrium thickness (respectively, 10 and 8 mm on average for the PRP and estradiol groups) enabled FET in all cases. The PRP therapy afforded higher rates of clinical pregnancy and live births (14% vs 6%) against a backdrop of lower occurrence of miscarriages (3% versus 6%) compared with the estradiol therapy (Coksuer, Akdemir & Ulas Barut, 2019). In study of Kim et al., intrauterine administration of the autologous PRP also improved implantation and pregnancy outcomes for the patients with the refractory thin endometrium-associated infertility which indicates profound functional consistency of its effects (Kim et al., 2019).

Endometrium is a dynamic structure composed of simple columnar epithelium with uterine glands, and the underlying stroma (Pertschuk, 1990) with blood vessels, nerves, collagen and reticular fibers, and a variety of stromal cells (Aplin, 2018). Isolation of mesenchymal stem/stromal cells (MSCs) from endometrium (Chan, Schwab & Gargett, 2004; Chan & Gargett, 2006) allows elucidation of tissue-specific functions and markers of these cells thus opening new prospects of their usage. As actively proliferating cells, MSCs play an important role in the tissue homeostasis of endometrium — they are involved in the extracellular matrix remodeling, angiogenesis, cell-to-cell communication, post-menstrual tissue repair, etc.(Mutlu, Hufnagel & Taylor, 2015; Arutyunyan et al., 2016). Endometrial stromal cells are highly susceptible to the action of PRP (Matsumoto et al., 2005); however, only a few works are devoted to studying of exact mechanisms of PRP action on these cells (Aghajanova et al., 2018). The use of rat endometrial MSCs makes a good model for studying the action of PRP in the perspective of

infertility treatment due to the ethical accessibility and sufficient size of the biomaterial which allows to obtain more cells than from human pipe endometrial biopsy (Jang et al., 2017).

Experimental animal models are accessible and provide better uniformity of samples. The use of human biomaterial is invariably associated with heterogeneity of anamneses and preliminary treatment regimens, the use of different collection protocols. Moreover, in the cases of thin endometrium, the diagnostic curettage is strongly contraindicated and substituted with pipe biopsies which provide very limited sample volumes insufficient for the comprehensive examination.

MSCs isolated from the rat uterus represent an available counterpart to the MSCs of human endometrium. The uterine tissues were preferred to the conventional sources of MSCs (including the red bone marrow, adipose tissue and umbilical cord) because of the significant difference in functional properties of MSCs isolated from different locations in the body. For example, MSCs isolated from adipose tissue show higher proliferation rates and a higher adipogenic differentiation capacity than MSCs isolated from the red bone marrow (Brown et al., 2019). At the same time, the bone marrow-derived MSCs are more prone to osteogenic differentiation, whereas MSCs isolated from muscle tissue show the highest rates of differentiation into myogenic progeny and express myoblastic markers (Brown et al., 2019). Despite the common immunophenotype signatures of MSCs isolated from different tissue sources (they express CD73, CD90, and CD105 and do not express hematopoietic markers CD34 and CD45 at their surface), these cells also exhibit a number of tissue-specific surface markers (Klimczak & Kozlowska, 2016), which implicates the tissue-dependent functional specificity.

In this study, we examine the effects of autologous PRP on the MSCs isolated from rat uterus and compare them with the effects of autologous ordinary plasma (OP).

Materials & Methods

Ethical disclosure

The authors state that they have obtained appropriate institutional review board approval or have followed the principles outlined in the Declaration of Helsinki for all human or animal experimental investigations. The study was approved by the Ethical Review Board at the Scientific Research Institute of Human Morphology (Protocol №.15, 9th of December, 2019).

Animals. The outbred eight-week-old female Sprague-Dawley rats of 250–300 g weight were obtained from the Institute for Bioorganic Chemistry branch animal facilities (Pushchino, Moscow region, Russia). All experimental work involving animals was carried out according to the standards of laboratory practice (National Guidelines No. 267 by Ministry of Healthcare of the Russian Federation, June 1, 2003), and all efforts were made to minimize the suffering. The animals were adapted to the laboratory conditions (23°C, 12 h/12 h light/dark, 50% humidity, and ad libitum access to food and water) for 2 weeks prior to the experiments. In adult female rats, the stage of the estrous cycle was determined by taking a vaginal smear. The smear was stained with methylene blue and the stage was determined by assessment of cellular composition of the smear. The uterus was dissected at the stage of metestrus after the euthanasia in a CO_2-chamber; the blood was collected by puncture from the heart. Animals served only as a source of the uterus and autologous plasma; therefore, no experimental conditions and endpoints were used.

PRP and OP preparation. The blood was collected in tubes with 2 ml of heparin (5000 IU/ml) and 800 µl of 10% sodium citrate. An average of 6 ml of blood was obtained from one animal. PRP was obtained based on a protocol developed by Yazigi et al. (Yazigi Junior et al., 2015). The blood was centrifuged at 400 g for 10 min, the plasma was collected in a new tube and

centrifuged again at 4 °C, 400 g for 10 min. After centrifugation, 70% of the supernatant (the platelet-poor plasma, PPP) was discarded. The remaining fraction PRP, which according to the modern classification belongs to L type (L-PRP), was preserved. The platelet counts were determined on a TC20 Automated Cell Counter (Bio-Rad, USA) and constituted 50×10^6 platelets/ml on average. To obtain OP, the blood was centrifuged at 4 °C, 2000 g for 15 min, and the supernatant was collected. The prepared OP and PRP were aliquoted, frozen and stored at -20 °C. Before use, PRP was activated by adding 10% $CaCl_2$ (10 µl of per 200 µl of PRP) according to the protocol by Messora et al.(Messora et al., 2011)

The protocol for obtaining MSCs from rat endometrium. The primary cell cultures were obtained based on the protocol by De Clercq et al. with modifications (De Clercq, Hennes & Vriens, 2017). The dissected uterus was minced with scissors in Hank's Balanced Salt Solution (HBBS) and transferred into 0.25% trypsin. The tube was incubated at 4 °C for 1 h, then at 22 °C for 1 h, and finally at 37 °C for 15 min with periodical shaking. The supernatant was taken and the solid bulk was transferred to a solution of collagenases type I and type IV in 0.05% trypsin-EDTA solution (collagenase I:collagenase IV:trypsin-EDTA, 1:1:10), incubated at 37 °C for 30 min, and passed through a 70 µm cell strainer. The material remaining on the strainer was transferred to a fresh solution of collagenases with 0.05% trypsin-EDTA, incubated at 37 °C for 15 min, and passed through a strainer again. The resulting suspension containing the cells of interest was centrifuged at 300 g for 5 min at 22 °C. The pellet was resuspended in HBBS supplemented with 1% FBS, centrifuged again, and resuspended in complete growth medium (DMEM/F-12 supplemented with 10% FBS, L-glutamine and penicillin/streptomycin) for cultivation. The obtained cells were verified for compliance with the minimal criteria for MSCs issued by the International Society for Cellular Therapy (Dominici et al., 2006) (adhesion to

untreated plastic, specific profile of surface antigens, and *in vitro* differentiation towards osteogenic, chondrogenic and adipogenic progeny). To assess the effects of PRP and OP on MSCs, the cells were cultured for 24 h in the medium supplemented with 10% PRP and 10% OP, respectively, instead of FBS. Complete growth medium (CGM) with 10% FBS was used as the control.

Flow cytometry analysis. Immunophenotyping of the cells for the surface and intracellular markers was performed upon reaching 80% confluence. The harvested cells were centrifuged at 800 g for 10 min, the supernatant was discarded, the cells were fixed in 2% paraformaldehyde for 15 min at room temperature (RT), diluted with 5 ml of PBS, and centrifuged at 1500 g for 10 min. The pellet was resuspended in 1 ml of PBS. For immunostaining, 1×10^5 of fixed cells cells were incubated in 100 µl of Rinsing Solution (Miltenyi Biotec, USA) with primary antibodies to CD90 (ab225, 1/100, Abcam), CD45 (130-107-846, clone REA504, 1/20, Miltenyi Biotec), CD105 (ab107595, 1/100, Abcam), CD34 (PAB18289, 1/100, Abnova) at room temperature for 1 h, and subsequently with secondary antibodies — anti-mouse Ig-FITC (ab6785, 1/500, Abcam) or anti-rabbit Ig-PE (sc-3739, 1/100, Santa Cruz) at RT for 1 h in the dark. After the incubation, the cells were washed in PBS, resuspended in 0.5 ml of PBS, and transferred to fresh tubes for the analysis on a FACScan flow cytometer (Becton Dickinson, USA) with the CellQuest software.

Induced differentiation of MSCs. The ability of MSCs to differentiate in osteo-, chondro- and adipogenic directions was assessed at early passages (up to 7). The cells were grown to 70% confluency in CGM, and then the growth medium was replaced with differentiation medium (for differentiation) or CGM (for the controls). Differentiation into adipogenic progeny was accomplished by using StemPro® Adipogenesis Differentiation Kit (Gibco) in the course of 7

days. At the end of the differentiation process, the cells were fixed with ethyl alcohol:formalin solution (1:4) for 3 minutes and stained with Sudan III (5.7 mM) for 10 minutes to visualize fat droplets. For osteogenic differentiation, the medium was supplemented with dexamethasone (10^{-7} M) and ascorbic acid (0.2 mM) in the course of two weeks. At the end, the cells were fixed with 70% alcohol, and for the detection of mineralization sites, the cells were stained with 40 mM alizarin red S solution (pH = 4.7) for 5 min. Chondrogenic differentiation was performed by using StemPro® Chondrogenesis Differentiation Kit (Gibco). After two weeks of differentiation, the cells were fixed with 4% formalin for 1 h and for detection of mucopolysaccharides were stained with 1% alcian blue for 24 h. Samples were analyzed using an Axiovert 40 CFL inverted microscope (Zeiss, Germany) using ZEN software (Carl Zeiss, Germany).

Immunocytochemistry. The MSCs were grown on glass coverslips (Fisher Scientific) coated with gelatin and placed in Petri dishes (35 × 10 mm). For immunocytochemistry, the cells were fixed in 2% paraformaldehyde. The coverslips with fixed cells were treated with 0.1% Triton X-100 for 10 min (cell membrane permeabilization) and washed with PBS. Non-specific binding sites were blocked with 1% BSA in PBS with 0.1% Tween-20 for 30 minutes. The coverslips were incubated with antibodies to Ki-67 (ab15580, 1/100, Abcam) or vimentin (ab8978, 1/250, Abcam) at +4 °C for 24 hours. After incubation, the coverslips were washed with PBS and then incubated with the secondary anti-rabbit-PE antibodies (1/200) or anti-rabbit-FITC antibodies (1/200) in the dark at RT for 1 h and subsequently washed with PBS. To stain the nuclei, the coverslips were incubated with DAPI (0.004 mg / ml) at 37 °C for 10 min. Then the coverslips were washed in PBS and mounted in Aqua-Poly Mount (Polysciences, USA). The photographs were made using a Leica DM 4000B fluorescence microscope (Leica Microsystems, Germany) with the LAS AF v.3.1.0 software (Leica Microsystems, Germany).

Western blot assay. The cells were washed with PBS and lysed in the ice-cold RIPA buffer. The sample was mixed with 2X loading buffer and incubated at 95 °C for 1 minute. The samples were stored at -80 °C until use and heated for 1 min at 95 °C before loading. The proteins were separated by 10–12.5% sodium dodecyl sulfate polyacrylamide gel electrophoresis (SDS-PAGE) and transferred from the gel to PVDF membranes by the semi-wet approach using Trans-Blot® Turbo™ RTA Mini LF PVDF TransferKit (Bio-Rad Laboratories, Inc.). The membranes were blocked with 5% milk in Tris-buffered saline containing 0.1% Tween (TTBS) at RT for 1 h, then stained overnight with primary antibodies to LC3B (1:3000, ab48394, Abcam), Bcl-2 (1:1000, ab32124, Abcam), p53 (1:250, ab90363, Abcam), ERα (1:2000, ab3575, Abcam), MMP-9 (1:1000, ab38898, Abcam) and GAPDH (1:500, sc-25778, Santa Cruz) and subsequently with the HRP-conjugated secondary antibodies (1:5000, Bio-Rad Laboratories, Inc.). Chemiluminescent signal developed by using Novex ECL Kit (Invitrogen, USA) was visualized in a C-DiGit® Blot Scanner (LI-COR, USA) using the Image Studio™ Acquisition Software (LI-COR, USA). Figure of uncropped membrane is available in Supplementary information (Fig.S1). The relative protein levels were determined via normalization by GAPDH signals. The bands represent biological replicates (i.e. correspond to different individuals).

Statistical analysis. Statistical data processing was performed in the GraphPad Prism 8 (Software GraphPad Software, USA). The Shapiro-Wilk test was applied to assess the normality of distributions. In the case of normal distribution, one-way ANOVA with the Turkey post-hoc test for multiple comparison was used. In the case of non-normal distribution, the Kruskal-Wallis test with the post-hoc Dunn test was used. The differences were considered statistically significant at $p < 0.05$.

Results

Characterization of the isolated MSCs. The uterus is a non-classical source of MSCs. Given the wide variability of MSC phenotypes and tissue-specific features (Kwon et al., 2016), the first stage of our study was to show the compliance of rat uterine mesenchymal cell cultures to the established minimal criteria for MSCs, including the immunophenotype and the capability of induced *in vitro* differentiation into different mesenchymal lineages. The obtained cultures of fibroblast-like cells were immunophenotyped by flow cytometry for CD90, CD105, CD45 and CD34. The region of interest was selected by relation of forward and side scattering values in a FSC-SSC dot plot diagram (Figure 1 a) reflecting the size and granularity of the cells, respectively. We gated the major pool of single cell events (R1) excluding debris (Figure 1 a). The peaks of fluorescence were distinctly shifted in histograms for the MSC samples stained specifically with antibodies to CD90 and CD105 compared with the controls stained with secondary antibodies only (Figure 1 b, green curve). We found that 72.7% of the cells were positive for CD90 and 31.8% of the cells were positive for CD105, which indicated correspondence of the obtained cultures to the CD90+CD105+ phenotype. Interestingly, 3.1% and 20.1% of the cells were positive for CD45 and CD34, respectively. To further confirm the compliance, we stained the cultures for vimentin. The immunocytochemical assay revealed the presence of vimentin protein in 100% of the cells (Figure 1 c).

We promoted differentiation of the cell cultures into adipogenic, osteogenic and chondrogenic lineages by using specific combinations of inducers. The adipogenic differentiation was identified by formation of lipid droplets revealed by staining with Sudan III (Figure 1 d, left panel). During the osteogenic differentiation, the cells formed characteristic conglomerates, with the foci of calcification revealed by alizarin red staining (Figure 1 d, central panel). During the chondrogenic differentiation, conglomerates were also formed by the cells, and the

mucopolysaccharide production was revealed by staining with alcian blue (Figure 1 d, right panel).

Effects of autologous PRP and OP on cell proliferation and cell death. Effects of autologous PRP and OP on the rat uterine MSC cultures were evaluated after 24 h incubation of the cells in a medium containing 10% PRP or 10% OP instead of FBS. Accordingly, complete growth medium (CGM) with 10% FBS was used as a control. Proliferation was assessed by immunocytochemical staining for Ki-67 following the incubation (Figure 2 a). The percentage of Ki-67 positive nuclei divided by the total number of nuclei (proliferation index) was 18.1% for CGM, 41.9% for PRP, and 21.7% for OP (Figure 2 b). For PRP, the differences were statistically significant ($p = 0.04$).

To evaluate the activation or inhibition of apoptosis, we analyzed the production of the stress-induced protein p53 and the anti-apoptotic protein Bcl-2. The p53 protein levels were significantly higher in the cells exposed to OP ($p = 0.03$), as compared with the control (Figure 2 c, d). After PRP exposure p53 production level did not change. Relative levels of Bcl-2 production did not differ among the studied groups (Figure 2 c, e).

Autophagy was assessed by the level of production of the autophagy marker LC3B. Western blot analysis revealed elevated production of LC3B protein in the cells exposed to autologous PRP, as compared with the control (CGM, Figure 2 c, f); the observed effect was statistically significant.

Endometrium receptivity: effects of autologous PRP and OP on the matrix metalloproteinase 9 (MMP9) and estrogen receptor α (ERα) production. Zinc-metalloproteinase MMP9 participates in the extracellular matrix remodeling. We estimated potential invasiveness of MSCs as a correlate of MMP9 production. Although elevated levels of

MMP9 production were observed in both OP and PRP groups compared to CGM, only in the OP treated cultures the MMP9 upregulation was significant ($p = 0.03$, Figure 3 a, b). In addition, we compared the levels of ERα, which can be partially associated with endometrial receptivity (Figure 3 c, d). Despite the elevated ERα levels in the PRP and OP treated cultures, the differences were not significant.

Discussion

Administration of PRP for the treatment of thin endometrium has been already introduced to clinical practice in a pilot study by Kim et al. aimed at increasing the endometrium thickness and accordingly the probability of implantation (Kim et al., 2019). However, the exact mechanism of the positive effect of PRP on the endometrium thickness remains obscure. In this study, we attempt to identify signaling pathways activated in the multipotent stromal cells of endometrium under the influence of autologous PRP by using rat endometrium as a model. Endometrial MSCs play a key role in the stroma: they participate in the regeneration of the functional layer of the endometrium due to the presence of receptors for sex hormones and the ability for extracellular matrix remodeling (Mutlu, Hufnagel & Taylor, 2015). These features emphasize the importance of MSCs for the receptivity of endometrium during the implantation period. We isolated primary cultures of stromal cells from the rat uterus and proved that these cells were essentially MSCs by their ability to differentiate in adipogenic, osteogenic and chondrogenic directions *in vitro*. Phenotypic profiles of the isolated primary cultures were compliant with the CD90+CD105+Vimentin+CD45-CD34- profiles established for MSCs. The presence of cells positive for the CD45 and CD34 markers can be explained by small admixture of hematopoietic cells and high vascularization of the endometrial stroma. Considering a precedent of the 81% CD34- for synovial fluid-derived MSCs and 97.5% CD34- for synovial membrane-derived

MSCs cultures classified as CD34 negative, we classify the obtained cultures as CD45 and CD34 negative. The percentage of cells positive for CD105 seems lower than it was expected; however, the published evidence indicates substantial variability of this parameter for MSCs isolated from different tissue sources (Ponnaiyan & Jegadeesan, 2014).

In the experiments with plasma treatment, the obtained MSCs were incubated for 24 h in the control medium (the DMEM/F-12 based complete growth medium with 10% FBS) or the medium supplemented with autologous 10% PRP or 10% OP instead of FBS. We observed increased proliferation rates of MSCs under the influence of PRP compared with the influence of FBS. This observation indicates mitogenic effects of PRP on stromal cells. We also studied the protein production levels for the established markers of apoptosis and autophagy. The stress-induced protein p53 is a transcription factor that regulates cell cycle and acts as a tumor suppressor (Labuschagne, Zani & Vousden, 2018). An important function of p53 is to prevent the accumulation of DNA damage. In the case of damage to cellular DNA, p53 promotes cell cycle arrest and triggers the emergency DNA repair systems; in the case of extensive DNA damage, p53 triggers apoptosis (Wang, Simpson & Brown, 2015). We show that OP promotes increased production of p53 protein by stromal cells, revealing a certain degree of cellular stress associated with the OP treatment. At the same time, both PRP and OP have no effects on the levels of the anti-apoptotic Bcl-2 protein production by MSCs. Bcl-2 is anti-apoptotic protein localized on the outer mitochondrial membrane, as well as the membranes of nuclear envelope and endoplasmic reticulum (Delbridge et al., 2016). Apparently, Bcl-2 activation is not involved in the effects of PRP and OP.

We used LC3B as an autophagy marker — this protein is involved in the biogenesis of autophagosomes (Barth, Glick & Macleod, 2010). Upon binding to the membrane, LC3

conjugates with phosphatidylethanolamine lipid (Tanida, Ueno & Kominami, 2008). After the autophagosome formation, LC3-II located in the outer layer is released into the cytosol, while LC3-II located in the inner layer is exposed to hydrolases. LC3B-II is conventionally used as a marker of autophagosomal activity. We observed excessive production of LC3B in MSCs after the exposure to PRP. This observation suggests that PRP contribute to self-renewal of the endometrial stromal cells by enhancing autophagy. The rapamycin-induced autophagy was shown to enhance the viability of MSCs, while shRNA-mediated knockdown of the autophagy-associated genes decreased their viability (Molaei et al., 2015; Jakovljevic et al., 2018). The decreased autophagy levels are currently considered as one of the mechanisms underlying the aging of MSCs (Fafián-Labora, Morente-López & Arufe, 2019).

Endometrial receptivity results from a combination of different characteristics of the endometrium responsible for the ability to promote implantation. One of the indicators of endometrial receptivity is the level of ERα, as it mediates the action of estrogens preparing the endometrium for implantation by increasing its thickness via the increase in the rates of cell proliferation. In clinical practice, the level of production of ERα can be evaluated by staining of endometrial cells with antibodies to ERα (Glasser et al., 2002), which is expressed by several subpopulations of endometrial stromal cells including MSCs (Zhou et al., 2001). We therefore employed ERα as a marker reflecting the conditional receptivity of endometrium in our model. We observed no significant differences in the level of ERα production upon exposure of the MSCs to PRP or OP, which may indicate that the beneficial effects of these agents are estrogen-independent. However, this finding should be verified on larger samples to exclude individual variations in the estrogen dependence of the plasma treatment effects.

Apart from sensitivity of the endometrium to the action of hormones, it should be susceptible and supportive to the trophoblast invasion. The trophoblast cells bind to the endometrium, proliferate and penetrate deep into the stroma to come into contact with the maternal blood (Bischof, Meisser & Campana, 2000). Progressive remodeling of the extracellular matrix is a hallmark of this process (Bischof, Meisser & Campana, 2002). Expression of matrix metalloproteinases, observed not only in the trophoblast but also in the endometrial stromal cells, provides effective support to the trophoblast invasion (Bischof, Meisser & Campana, 2002). In this study, we used MMP9 production as an indicator of the MSC capacity for extracellular matrix remodeling, which is an important parameter of morphogenetic plasticity and receptivity of the endometrium. We demonstrated an increase in the MMP9 production specifically facilitated by OP as compared to CGM.

In general, the obtained results indicate stimulatory effects of PRP on the endometrium, as indicated by behavior of MSCs isolated from it. Some other studies also indicate that PRP enhances cell proliferation and differentiation in the uterus (Aghajanova et al., 2018; Etulain et al., 2018). Intrauterine administration of PRP to the rats with damaged endometrium enhanced proliferation thus promoting tissue repair and also reducing fibrosis (Jang et al., 2017).

In the study by Kim and et al. the therapeutic effect of PRP in the treatment of Asherman's syndrome on a mouse model was demonstrated (Kim et al., 2020). Asherman’s syndrome is characterized by formation of adhesions and fibrotic lesions inside the uterus. Injections of human PRP at the sites of damage reduced the degree of fibrosis and promoted the recovery. It was shown that after PRP therapy implantation potential substantially increased and 83.3% of PRP-treated mice gave birth to live offspring compared to the 0.0% in the control group.

The receptivity of endometrium strongly depends on the inflammatory status and favorable antimicrobial conditions. Pronounced anti-inflammatory effects of PRP on the endometrium in horses were demonstrated by Reghini et al. (Reghini et al., 2016). Uterine infusions of PRP to mares with chronic endometritis significantly reduced the signs of neutrophilic infiltration and the volume of intrauterine fluid accumulation as observed at 24 h after the treatment (Reghini et al., 2016). The mechanisms of PRP action on the endometrial cells are still disputable and apparently involve anti-inflammatory and pro-proliferative signaling.

The effects of OP on endometrium are notably understudied. In our experiments, OP induced up-regulation of the p53 and MMP9 protein expression so the beneficial effects of OP are less pronounced. The growth factors released from the PRP activated platelets stimulate proliferation of endometrial cells and enhance autophagy which indicates the advantages of PRP as a treatment agent for the endometrial dysfunction.

Conclusions

The use of modified blood plasma for clinical applications is expanding. This study evaluates the effects of the autologous platelet-rich plasma (PRP) and ordinary plasma (OP) on tissue-specific MSCs from rat endometrium. Exposure to PRP enhances proliferation of the uterine MSCs with a significant increase in autophagy. Exposure to OP increased the production of the stress-induced protein p53 and extracellular enzyme MMP9. The results indicate the potency of PRP for the treatment of infertility, particularly for the management of thin endometrium. Understanding of molecular pathways mediating the beneficial effects of PRP will expand the range of PRP applications.

Acknowledgements

Special thanks to Natalia Usman for her help with proofreading of the manuscript.

References

Aghajanova L, Houshdaran S, Balayan S, Manvelyan E, Irwin JC, Huddleston HG, Giudice LC. 2018. In vitro evidence that platelet-rich plasma stimulates cellular processes involved in endometrial regeneration. *Journal of Assisted Reproduction and Genetics* 35:757–770. DOI: 10.1007/s10815-018-1130-8.

Aplin J. 2018. Uterus-endometrium. In: *Encyclopedia of Reproduction*. Elsevier, 326–332. DOI: 10.1016/B978-0-12-801238-3.64654-8.

Arutyunyan I V., Fatkhudinov TH, El'chaninov A V., Makarov A V., Kananykhina EY, Usman NY, Raimova ES, Goldshtein D V., Bol'shakova GB. 2016. Effect of Endothelial Cells on Angiogenic Properties of Multipotent Stromal Cells from the Umbilical Cord during Angiogenesis Modeling in the Basement Membrane Matrix. *Bulletin of Experimental Biology and Medicine* 160:575–582. DOI: 10.1007/s10517-016-3221-9.

Barth S, Glick D, Macleod KF. 2010. Autophagy: assays and artifacts. *The Journal of pathology* 221:117–24. DOI: 10.1002/path.2694.

Bischof P, Meisser A, Campana A. 2000. Mechanisms of endometrial control of trophoblast invasion. *Journal of reproduction and fertility. Supplement* 55:65–71.

Bischof P, Meisser A, Campana A. 2002. Control of MMP-9 expression at the maternal-fetal interface. In: *Journal of Reproductive Immunology*. Elsevier, 3–10. DOI: 10.1016/S0165-0378(01)00142-5.

Brown C, McKee C, Bakshi S, Walker K, Hakman E, Halassy S, Svinarich D, Dodds R, Govind CK, Chaudhry GR. 2019. Mesenchymal stem cells: Cell therapy and regeneration potential. *Journal of Tissue Engineering and Regenerative Medicine* 13:1738–1755. DOI: 10.1002/term.2914.

Cavallo C, Roffi A, Grigolo B, Mariani E, Pratelli L, Merli G, Kon E, Marcacci M, Filardo G. 2016. Platelet-Rich Plasma: The Choice of Activation Method Affects the Release of Bioactive Molecules. *BioMed Research International* 2016. DOI: 10.1155/2016/6591717.

Chan RWS, Gargett CE. 2006. Identification of Label-Retaining Cells in Mouse Endometrium. *STEM CELLS* 24:1529–1538. DOI: 10.1634/stemcells.2005-0411.

Chan RWS, Schwab KE, Gargett CE. 2004. Clonogenicity of Human Endometrial Epithelial and Stromal Cells1. *Biology of Reproduction* 70:1738–1750. DOI: 10.1095/biolreprod.103.024109.

Civinini R, Macera A, Nistri L, Redl B, Innocenti M. 2011. The use of autologous blood-derived growth factors in bone regeneration. *Clinical Cases in Mineral and Bone Metabolism* 8:25–31.

De Clercq K, Hennes A, Vriens J. 2017. Isolation of mouse endometrial epithelial and stromal cells for in Vitro decidualization. *Journal of Visualized Experiments* 2017. DOI: 10.3791/55168.

Coksuer H, Akdemir Y, Ulas Barut M. 2019. Improved in vitro fertilization success and pregnancy outcome with autologous platelet-rich plasma treatment in unexplained infertility patients that had repeated implantation failure history. *Gynecological Endocrinology* 35:815–818. DOI: 10.1080/09513590.2019.1597344.

Delbridge ARD, Grabow S, Strasser A, Vaux DL. 2016. Thirty years of BCL-2: Translating cell death discoveries into novel cancer therapies. *Nature Reviews Cancer* 16:99–109. DOI: 10.1038/nrc.2015.17.

450 Dominici M, Le Blanc K, Mueller I, Slaper-Cortenbach I, Marini FC, Krause DS, Deans
451 RJ, Keating A, Prockop DJ, Horwitz EM. 2006. Minimal criteria for defining
452 multipotent mesenchymal stromal cells. The International Society for Cellular
453 Therapy position statement. *Cytotherapy* 8:315–317. DOI:
454 10.1080/14653240600855905.
455 Etulain J, Mena HA, Meiss RP, Frechtel G, Gutt S, Negrotto S, Schattner M. 2018. An
456 optimised protocol for platelet-rich plasma preparation to improve its angiogenic
457 and regenerative properties. *Scientific Reports* 8:1–15. DOI: 10.1038/s41598-018-
458 19419-6.
459 Fafián-Labora JA, Morente-López M, Arufe MC. 2019. Effect of aging on behaviour of
460 mesenchymal stem cells. *World Journal of Stem Cells* 11:337–346. DOI:
461 10.4252/wjsc.v11.i6.337.
462 Flaumenhaft R, Sharda A. 2018. The life cycle of platelet granules. *F1000Research* 7.
463 DOI: 10.12688/f1000research.13283.1.
464 Frantz N, Ferreira M, Kulmann MI, Frantz G, Bos-Mikich A, Oliveira R. 2020. Platelet-
465 Rich plasma as an effective alternative approach for improving endometrial
466 receptivity - a clinical retrospective study. *JBRA Assisted Reproduction*. DOI:
467 10.5935/1518-0557.20200026.
468 Glasser SR, Aplin JD, Giudice LC, Tabibzadeh S. 2002. *The endometrium*. Taylor &
469 Francis.
470 Jakovljevic J, Harrell CR, Fellabaum C, Arsenijevic A, Jovicic N, Volarevic V. 2018.
471 Modulation of autophagy as new approach in mesenchymal stem cell-based
472 therapy. *Biomedicine and Pharmacotherapy* 104:404–410. DOI:
473 10.1016/j.biopha.2018.05.061.
474 Jang HY, Myoung SM, Choe JM, Kim T, Cheon YP, Kim YM, Park H. 2017. Effects of
475 autologous platelet-rich plasma on regeneration of damaged endometrium in
476 female rats. *Yonsei Medical Journal* 58:1195–1203. DOI:
477 10.3349/ymj.2017.58.6.1195.
478 Kim MH, Byeon HS. 2019. Review for good platelet-rich plasma procedure in cosmetic
479 dermatology and surgery. *Journal of Cosmetic Medicine* 3:1–13. DOI:
480 10.25056/jcm.2019.3.1.1.
481 Kim JH, Park M, Paek JY, Lee WS, Song H, Lyu SW. 2020. Intrauterine Infusion of
482 Human Platelet-Rich Plasma Improves Endometrial Regeneration and Pregnancy
483 Outcomes in a Murine Model of Asherman's Syndrome. *Frontiers in Physiology*.
484 DOI: 10.3389/fphys.2020.00105.
485 Kim H, Shin JE, Koo HS, Kwon H, Choi DH, Kim JH. 2019. Effect of autologous platelet-
486 rich plasma treatment on refractory thin endometrium during the frozen embryo
487 transfer cycle: A pilot study. *Frontiers in Endocrinology* 10. DOI:
488 10.3389/fendo.2019.00061.
489 Klimczak A, Kozlowska U. 2016. Mesenchymal stromal cells and tissue-specific
490 progenitor cells: Their role in tissue homeostasis. *Stem Cells International*. DOI:
491 10.1155/2016/4285215.
492 Kwon A, Kim Y, Kim M, Kim J, Choi H, Jekarl DW, Lee S, Kim JM, Shin JC, Park IY.
493 2016. Tissue-specific differentiation potency of mesenchymal stromal cells from
494 perinatal tissues. *Scientific Reports*. DOI: 10.1038/srep23544.
495 Labuschagne CF, Zani F, Vousden KH. 2018. Control of metabolism by p53 – Cancer

and beyond. *Biochimica et Biophysica Acta - Reviews on Cancer* 1870:32–42. DOI: 10.1016/j.bbcan.2018.06.001.

Lee D-H, Sonn CH, Han S-B, Oh Y, Lee K-M, Lee S-H. 2012. Synovial fluid CD34− CD44+ CD90+ mesenchymal stem cell levels are associated with the severity of primary knee osteoarthritis. *Osteoarthritis and Cartilage* 20:106–109. DOI: 10.1016/j.joca.2011.11.010.

Lubkowska A, Dolegowska B, Banfi G. 2012. Growth factor content in PRP and their applicability in medicine. *Journal of biological regulators and homeostatic agents*.

Maffulli N. 2016. *Platelet rich plasma in musculoskeletal practice*. DOI: 10.1007/978-1-4471-7271-0.

Marx RE. 2019. In Situ Tissue Engineering. In: Melville J, Shum J, Young S, Wong M eds. *Regenerative Strategies for Maxillary and Mandibular Reconstruction*. Springer International Publishing, 73–86. DOI: 10.1007/978-3-319-93668-0_7.

Marx RE, Carlson ER, Eichstaedt RM, Schimmele SR, Strauss JE, Georgeff KR. 1998. Platelet-rich plasma: Growth factor enhancement for bone grafts. *Oral Surgery, Oral Medicine, Oral Pathology, Oral Radiology, and Endodontics*. DOI: 10.1016/S1079-2104(98)90029-4.

Matsumoto H, Nasu K, Nishida M, Ito H, Bing S, Miyakawa I. 2005. Regulation of Proliferation, Motility, and Contractility of Human Endometrial Stromal Cells by Platelet-Derived Growth Factor. *The Journal of Clinical Endocrinology & Metabolism* 90:3560–3567. DOI: 10.1210/jc.2004-1918.

Messora MR, Nagata MJH, Furlaneto FAC, Dornelles4 RCM, Bomfim SRM, Deliberador TM, Garcia VG, Bosco AF. 2011. A standardized research protocol for platelet- rich plasma (PRP) preparation in rats. *RSBO Revista Sul-Brasileira de Odontologia*.

Molaei S, Roudkenar MH, Amiri F, Harati MD, Bahadori M, Jaleh F, Jalili MA, Roushandeh AM. 2015. Down-regulation of the autophagy gene, ATG7, protects bone marrow-derived mesenchymal stem cells from stressful conditions. *Blood Research* 50:80–86. DOI: 10.5045/br.2015.50.2.80.

Mutlu L, Hufnagel D, Taylor HS. 2015. The Endometrium as a Source of Mesenchymal Stem Cells for Regenerative Medicine1. *Biology of Reproduction* 92. DOI: 10.1095/biolreprod.114.126771.

Patel AN, Selzman CH, Kumpati GS, McKellar SH, Bull DA. 2016. Evaluation of autologous platelet rich plasma for cardiac surgery: Outcome analysis of 2000 patients. *Journal of Cardiothoracic Surgery* 11. DOI: 10.1186/s13019-016-0452-9.

Pertschuk LP. 1990. *Immunocytochemistry for steroid receptors*. CRC Press.

Ponnaiyan D, Jegadeesan V. 2014. Comparison of phenotype and differentiation marker gene expression profiles in human dental pulp and bone marrow mesenchymal stem cells. *European Journal of Dentistry* 8:307–313. DOI: 10.4103/1305-7456.137631.

Reghini MFS, Ramires Neto C, Segabinazzi LG, Castro Chaves MMB, Dell'Aqua C de PF, Bussiere MCC, Dell'Aqua JA, Papa FO, Alvarenga MA. 2016. Inflammatory response in chronic degenerative endometritis mares treated with platelet-rich plasma. *Theriogenology* 86:516–522. DOI: 10.1016/j.theriogenology.2016.01.029.

Tanida I, Ueno T, Kominami E. 2008. LC3 and Autophagy. In: Deretic V ed. *Autophagosome and Phagosome*. Totowa, NJ: Humana Press, 77–88. DOI: 10.1007/978-1-59745-157-4_4.

542 Theoret CL, Stashak TS. 2014. Integumentary System: Wound Healing, Management,
543 and Reconstruction. In: Orsini J, Divers T eds. *Equine Emergencies*. Elsevier Inc.,
544 238–267. DOI: 10.1016/b978-1-4557-0892-5.00019-2.
545 Wang X, Simpson ER, Brown KA. 2015. p53: Protection against tumor growth beyond
546 effects on cell cycle and apoptosis. *Cancer Research* 75:5001–5007. DOI:
547 10.1158/0008-5472.CAN-15-0563.
548 Yazigi Junior JA, dos Santos JBG, Xavier BR, Fernandes M, Valente SG, Leite VM.
549 2015. Quantification of platelets obtained by different centrifugation protocols in
550 SHR rats. *Revista Brasileira de Ortopedia (English Edition)* 50:729–738. DOI:
551 10.1016/j.rboe.2015.10.008.
552 Yuksel EP, Sahin G, Aydin F, Senturk N, Turanli AY. 2014. Evaluation of effects of
553 platelet-rich plasma on human facial skin. *Journal of Cosmetic and Laser Therapy*
554 16:206–208. DOI: 10.3109/14764172.2014.949274.
555 Yun SH, Sim EH, Goh RY, Park JI, Han JY. 2016. Platelet activation: The mechanisms
556 and potential biomarkers. *BioMed Research International*. DOI:
557 10.1155/2016/9060143.
558 Zadehmodarres S, Salehpour S, Saharkhiz N, Nazari L. 2017. Treatment of thin
559 endometrium with autologous platelet-rich plasma: A pilot study. *Jornal Brasileiro*
560 *de Reproducao Assistida* 21:54–56. DOI: 10.5935/1518-0557.20170013.
561 Zhou S, Zilberman Y, Wassermann K, Bain SD, Sadovsky Y, Gazit D. 2001. Estrogen
562 modulates estrogen receptor α and β expression, osteogenic activity, and
563 apoptosis in mesenchymal stem cells (MSCs) of osteoporotic mice. *Journal of*
564 *Cellular Biochemistry* 81:144–155. DOI: 10.1002/jcb.1096.
565

Figure 1

Characterization of the mesenchymal cell cultures isolated from rat uterus.

Flow cytometry analysis: a – representative forward and side scattering dot plot with the region of interest (R1). The percentages of CD90, CD105, CD45 and CD34 positive cells in R1 are indicated (b). Green curve corresponds to the control (stained with secondary antibodies only). Anti-vimentin staining (c): upper image – negative control (secondary antibodies only); lower image – immunocytochemistry with anti-vimentin antibodies (red) and the nuclei counterstained with DAPI (blue). Bars, 20 µm. Induced cell differentiation assay (d): adipogenic differentiation revealed by Sudan III staining, osteogenic differentiation revealed by alizarin red staining, and chondrogenic differentiation revealed by alcian blue staining. Upper panel – the non-induced control cells, bottom panel – cells after the induced differentiation. Bars, 50 µm. One experimental block is marked by a dotted line.

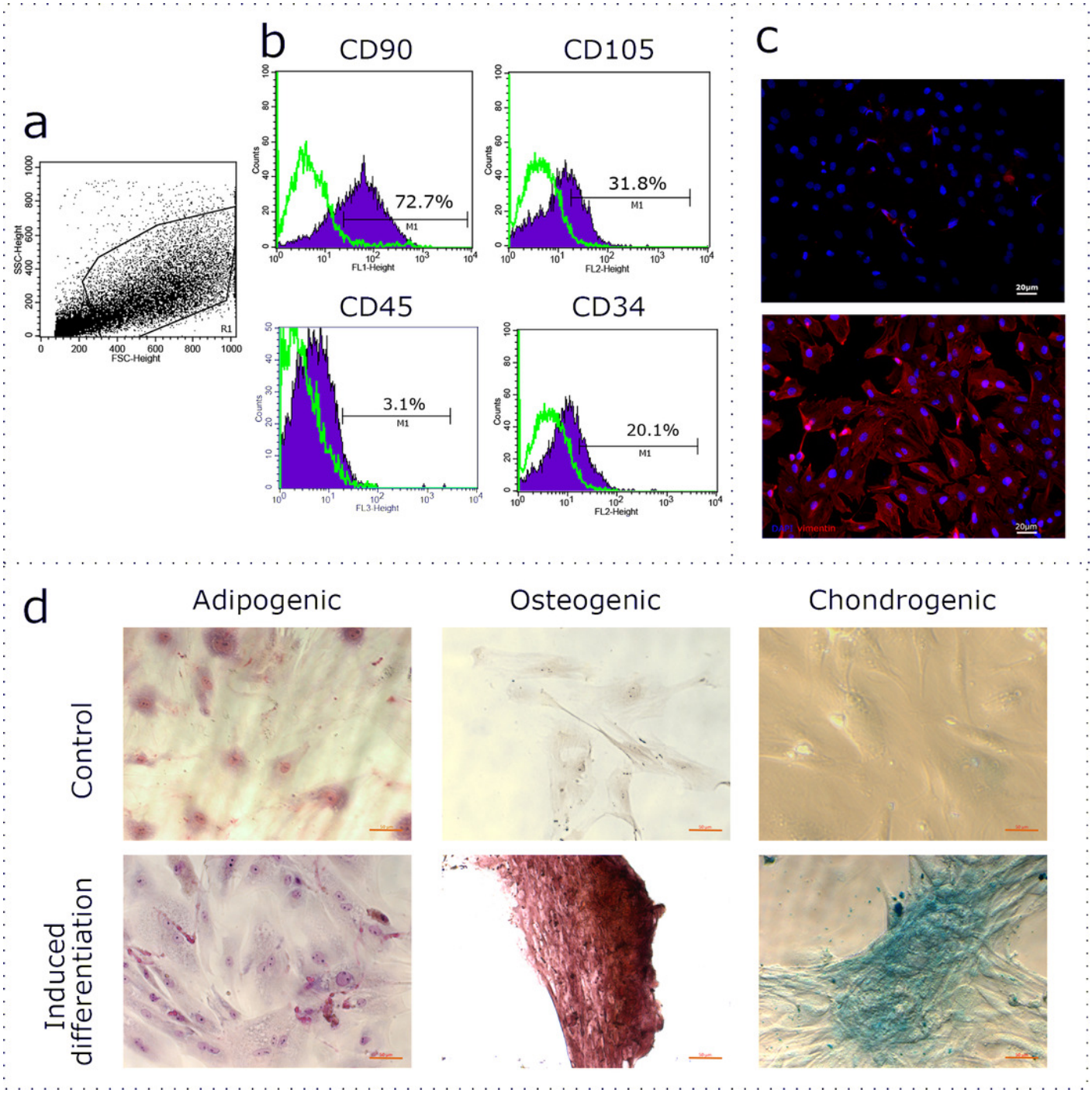
a
SSC-Height
FSC-Height
R1
b
CD90
72.7%
M1
FL1-Height
CD105
31.8%
M1
FL2-Height
CD45
3.1%
M1
FL3-Height
CD34
20.1%
M1
FL2-Height
Counts
c
20μm
DAPI vimentin
20μm
d
Adipogenic
Osteogenic
Chondrogenic
Control
Induced differentiation

Figure 2

The assessment of cell viability and cell death after the 24 h incubation of rat uterine MSCs with complete growth medium (CGM), platelet-rich plasma (PRP), or ordinary plasma (OP).

Immunocytochemical staining (a) for Ki-67 (green) after 24 h exposure of the MSC cultures to the CGM (left), PRP (central) and OP (right); the nuclei were counterstained with DAPI (blue). Bars, 20 μm. b – proliferation index calculated as the number of Ki-67 positive nuclei divided by the total number of nuclei. * - $p < 0.05$ vs CGM. c –representative western blot membranes with the proteins isolated from MSCs after 24 h incubation with the studied agents, stained with p53, Bcl-2, LC3B and GAPDH specific antibodies. Relative protein levels of p53 (d), Bcl-2 (e) and LC3B (f), normalized by GAPDH level. * - $p < 0.05$ vs CGM group. One experimental block is marked by a dotted line.

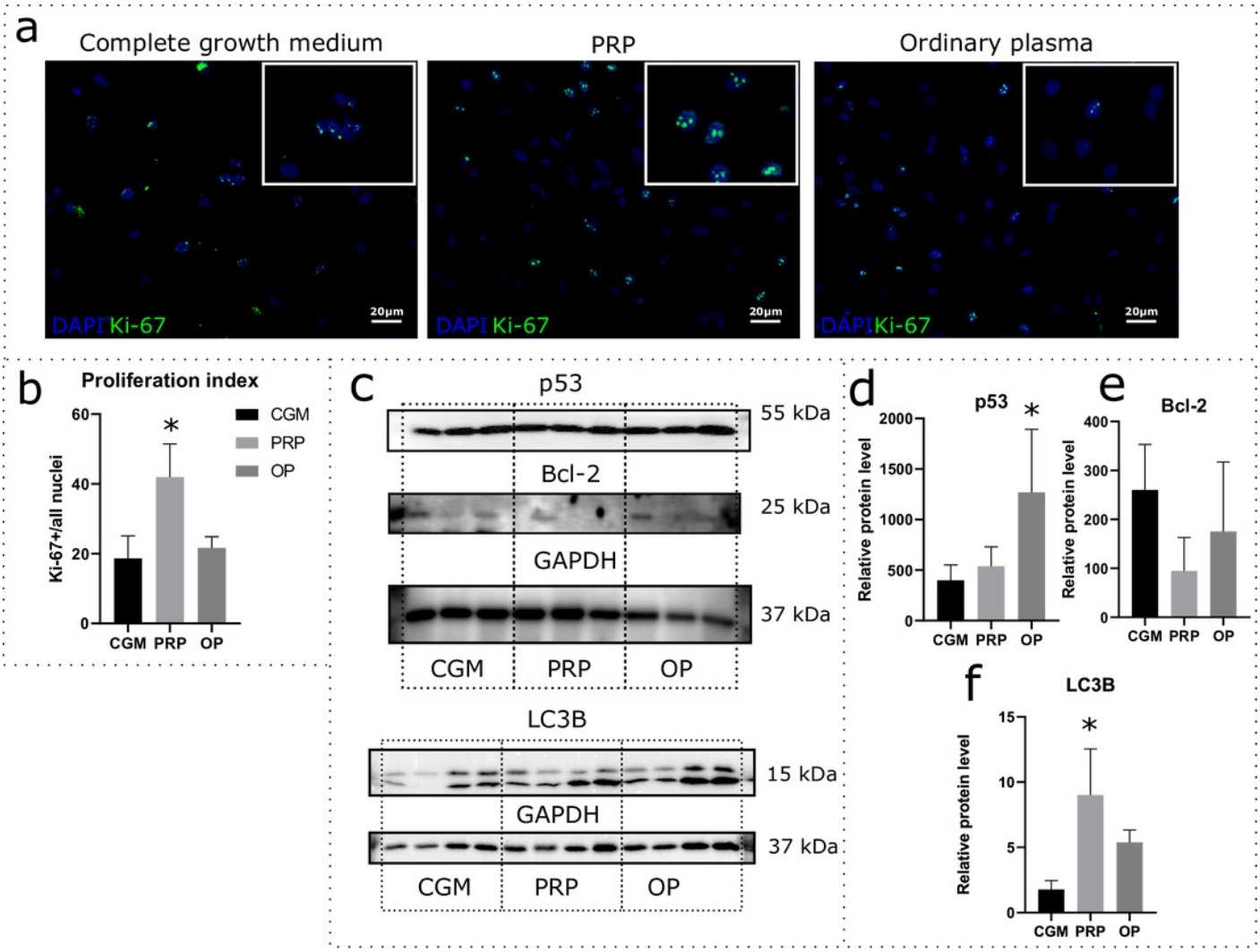
a
Complete growth medium
PRP
Ordinary plasma
DAPI Ki-67
20μm
b
Proliferation index
Ki-67+/all nuclei
CGM
PRP
OP
c
p53
55 kDa
Bcl-2
25 kDa
GAPDH
37 kDa
LC3B
15 kDa
d
p53
Relative protein level
e
Bcl-2
f
LC3B

Figure 3

Western blot membrane stained with MMP9 and ERα antibodies.

A representative western blot membrane with the proteins isolated from MSCs after 24 h incubation with complete growth medium (CGM), platelet-rich plasma (PRP) and ordinary plasma (OP), stained with MMP9 (a), ERα (c) and GAPDH specific antibodies. Relative protein levels of MMP9 (b) and ERα (d), normalized by GAPDH level. * - $p < 0.05$ vs CGM group.